Biosensors and Bioelectronics 26 (2011) 2506–2512

Contents lists available at ScienceDirect

Biosensors and Bioelectronics

journal homepage: www.elsevier.com/locate/bios

Construction of DNA biosensor at glassy carbon surface modified with 4-aminoethylbenzenediazonium salt

Agata Kowalczyk, Anna Nowicka, Rafal Jurczakowski, Michal Fau, Agata Krolikowska, Zbigniew Stojek*

Department of Chemistry, University of Warsaw, Pasteura 1, PL-02-093 Warsaw, Poland

ARTICLE INFO

Article history:
Received 1 September 2010
Received in revised form 20 October 2010
Accepted 25 October 2010
Available online 31 October 2010

Keywords:
DNA biosensors
DNA hybridization
4-Aminoethylbenzenediazonium salt
Carbon electrode
Electrochemical impedance spectroscopy
Raman spectroscopy

ABSTRACT

A simple, label-free electrochemical impedance-spectroscopy method for sequence-specific detection of DNA using a 4-aminoethylbenzenediazonium (AEBD) salt as a binder for amino-modified probe DNA is reported. This novel method simplifies the anchoring of DNA at the GC surface and opens new ways for the detection of hybridization. The hybridization of target DNA, without and with mismatches, with the probe DNA anchored at the GC surface modified with AEBD, greatly increases the interfacial electron transfer resistance at the double-stranded DNA modified electrodes for the redox couple $Fe(CN)_6^{3-/4-}$. The resistance was measured using electrochemical impedance spectroscopy. The sensor response increased linearly with logarithm of concentration of target DNA in the range $2 \times 10^{-12} \div 2 \times 10^{-6}$ M. The obtained quantification limit was circa 6.5×10^{-17} mole in a 7 μL droplet and corresponded to a concentration of 9.2×10^{-12} M of target DNA in the sample. This limit is equivalent to the detection of circa 4×10^7 copies of DNA in a 7 μL droplet or circa 5.7×10^{12} DNA copies in one litre of sample.

1. Introduction

Already for 20 years the appropriate modification of the conductive surfaces for the purpose of immobilization of such biomolecules as DNA and enzymes and finally for the purpose of construction of biosensors have been one of important aims in bioanalytical chemistry (Pividori et al., 2000; Gu and Hasebe, 2006). Carbon electrodes are very attractive as supports for (bio)sensors, because of their wide potential windows, good electrical conductivities and relatively low background currents. Several types of carbon have been applied as electric support/transducers for DNA hybridization biosensors: carbon paste (Wang et al., 1996), carbon fiber (Caruana and Heller, 1999), glassy carbon (Lin et al., 2007), highly oriented pyrolytic graphite (Hashimoto et al., 1994) and screen printed carbon (Marrazza et al., 1999). To accomplish high sensitivity and selectivity of a DNA biosensor the maximization of the hybridization efficiency and the minimization of nonspecific adsorption have to be achieved. Appropriate control of the surface chemistry and of coverage by probe DNA is essential for the success. So, the probe DNA immobilization step plays the major role in determination of the overall performance of an electrochemical DNA biosensor.

The simplest method to immobilize probe DNA at a carbon electrode surface is its adsorption at a controlled potential (Erdem et al., 1999; Palecek et al., 1993). However, this procedure leads to the existence of multiple sites of contact of the non-covalently bound probe DNA with the electrode surface, which results in poor hybridization efficiency. The immobilization of probe DNA at the carbon surface can be also obtained using the avidin–biotin based procedure (Campbell et al., 2002; Marrazza et al., 1999). The first step here was the formation of an avidin- or biotin layer onto the electrode surface and then the subsequent binding of the biotin or avidin modified oligonucleotides could take place.

Two efficient methods for the electrochemically assisted covalent modification of the carbon surfaces are known (Downard, 2000; Pinson and Podvorica, 2005). The first one is based on the electrochemical generation of the primary- or secondary amine radicals which are able to form covalent bonds with the carbon surface (Adenier et al., 2004; Gallardo et al., 2006; Tanaka and Aramata, 1997). The second method concerns the covalent bond between the organic molecule and the carbon electrode surface, which is formed by the electrochemical reduction of aryl diazonium salts (Actis et al., 2008; Downard, 2000; Ghanem et al., 2009).

In this study we propose a simple and rapid way to produce a stable, amino-derivatized conducting platform for creating a sensing layer in DNA biosensors. This can be achieved through the use of 4-aminoethylbenzenediazonium salt (AEBD) which can be immobilized on the glassy carbon surface via electroreduction. The presence of the terminal amino groups at the probe DNA

* Corresponding author. Tel.: +48 22 822 0211; fax: +48 22 822 4889.
E-mail addresses: anowicka@chem.uw.edu.pl (A. Nowicka), stojek@chem.uw.edu.pl (Z. Stojek).

0956-5663/$ – see front matter © 2010 Elsevier B.V. All rights reserved.
doi:10.1016/j.bios.2010.10.046

and the graphite surface can be used for the binding with the PEG molecules. The sensing layer created in this way and the final layer obtained after the hybridization process with a fully-complementary-, non-complementary- and mismatched target DNA were inspected by applying the electrochemical impedance spectroscopy (EIS) in the presence of the ferri/ferrocyanide redox indicator in the solution.

2. Materials and methods

2.1. Chemicals

All chemicals were of the highest quality available. NaOH (p.a., POCH, Poland), KH_2PO_4 (p.a., POCH, Poland), K_2HPO_4 (p.a., POCH, Poland), NaCl (p.a., POCH, Poland), KCl (p.a., POCH, Poland), tetrabutylammonium tetrafluoroborate (NBu_4BF_4; Sigma), acetonitrile (ACN dry, Aldrich, 99.8%), 4-(2-aminoethyl)aniline (Fluka, 97%), tetrafluorobric acid (p.a., POCH, Poland), sodium nitrite (p.a., POCH, Poland) and polyethylene glycol diglycidyl ether (PEG, MW 3350; Sigma) were used as received. All oligonucleotides used were purchased from MWG-Biotech (Germany). The following oligonucleatide sequences were used:

- probe DNA: (5′ → 3′): NH_2-C6-CGCCAACGTTTTCGCCAACG
- complementary target DNA (5′ → 3′): CGTTGGCGAAAACGTTG-GCG (designed from the gene of *Lactococcus*, a common milk bacteria)
- non complementary DNA strand (5′ → 3′): CGCCAACGTTTTCGC-CAACG
- single G-A mismatch DNA strand (5′ → 3′): CGTTAGC-GAAAACGTTGGCG
- single C-A mismatch DNA strand (5′ → 3′): CGTTGGA-GAAAACGTTGGCG
- double separated G-A mismatch DNA strand (5′ → 3′): CGTTAGC-GAAAACGTTGACG
- double neighbour G-A mismatch DNA strand (5′ → 3′): CGTTGGC-GAAAACGTTAACG

The synthesis of 4-aminoethylbenzenediazonium tetrafluoroborate (AEBD) was done according to the procedure described in the literature (Griveau et al., 2007). More details about synthesis are given in Supporting Information.

2.2. Electrochemical measurements

Cyclic voltammetry (CV) and electrochemical impedance spectroscopy (EIS) were performed using an Autolab, model PGSTAT 12 potentiostat equipped with an ECD amplifier module (RC time settings: 0 s for scan rates > 10 mV/s and 0.1 s for scan rates < 10 mV/s) and the electrochemical analysis system based on the GPES or FRA software package (Eco Chemie B.V., Utrecht, Netherlands). Impedance spectra were recorded for the frequency range 0.05 Hz ÷ 100 kHz with the ac amplitude equal to 10 mV (peak-to-peak). The fitting of the experimental data to the appropriate equivalent circuit was performed using the Complex Nonlinear Least-Squares (CNLS) method. For electrochemical measurement the three-electrode system consisting of a glassy carbon (GC) disc electrode (3 mm in diameter, BAS, UK) used as the working electrode, a reference electrode (Ag/AgCl/3 M KCl) and a platinum wire used as the auxiliary electrode were employed. The surface of the working electrode was polished with 1 and 0.3 μm Al_2O_3 powder on a wet pad. After each polishing, to remove alumina completely from the electrode surface, the electrode was rinsed with a direct stream of ultrapure water (Milli-Q, Millipore, conductivity of ~0.056 μS/cm) and dried with argon. In all experiments, the electrochemical cell was kept in a Faraday cage to minimize the electrical noise.

2.3. Raman spectroscopy

Raman spectra and maps were collected in the backscattering configuration with a Labram HR800 (Horiba Jobin Yvon) confocal microscope system equipped with a Peltier-cooled CCD detector (1024 × 256 pixel), using a 20 mW He–Ne (632.8 nm) laser. The confocal pinhole size was set to 200 μm and the holographic grating with 600-grooves/mm was used. The calibration of the instrument was performed using a 520 cm^{-1} Raman signal of a silicon wafer. All Raman spectra were obtained using a 50× magnification Olympus objective. Raman 3D mapping was performed on a 50 μm × 60 μm area with 4-μm resolution, for which the depth profile in a range of +5 μm ÷ −5 μm with a 2 μm step was acquired. The Raman spectra and maps were obtained and analyzed using the LabSpec5 software.

AEBD salt used for Raman measurements was sealed in a glass capillary, while GC/AEBD layer was sputtered with a gold layer of 2 nm thickness. Gold layers were prepared by vacuum sputtering from the pure Au target. The nominal thickness of the sputtered layers was estimated from the calibration curve of a Sputter Coater, Model SC7620 (Polaron).

2.4. AFM and contact angle measurements

AFM and contact angle measurements were done before and after modification of the glassy carbon surface by electroreduction of AEBD salt. Measurements of the contact angle were performed using a Hetta Lite Optical Fensiometer, model TL100. AFM pictures were obtained using a NanoScope IIIa instrument (Digital Instrument Santa Barbara). This allowed us to get qualitative characteristics of the AEBD layer.

2.5. Determination of affinity constant (K_a)

The Langmuir model is suitable for the treatment of interfacial DNA/DNA or PNA/DNA reactions (Kambhampati et al., 2001; Neumann et al., 2002). The determination of the K_a value for the hybridization process was based on the Langmuir adsorption isotherm, according to the formula (Liu et al., 2005):

$$R_{ct} = \frac{R_{ct\,max} C_o K_A}{1 + C_o K_A} \quad (1)$$

where R_{ct} is electron transfer resistance, $R_{ct\,max}$ – the maximal value of electron transfer resistance, and C_o – concentration of complementary target DNA.

A plot of C_o/R_{ct} vs. C_o yields a straight line from which the affinity constant can be calculated.

3. Preparation of biosensor

Each final measurement involved an immobilization/detection procedure at a freshly prepared glassy carbon disc electrode. All experiments were performed at room temperature (21 ± 1 °C). The preparation of the electrochemical DNA hybridization sensor involved several steps listed below and is illustrated in Fig. 1A.

3.1. Modification of electrode surface with AEBD salt (1)

One-electron reduction of AEBD salt at a GC electrode in ACN leads to grafting of the aryl groups to the surface. Five voltammetric reduction cycles are sufficient to get a satisfying organic layer.

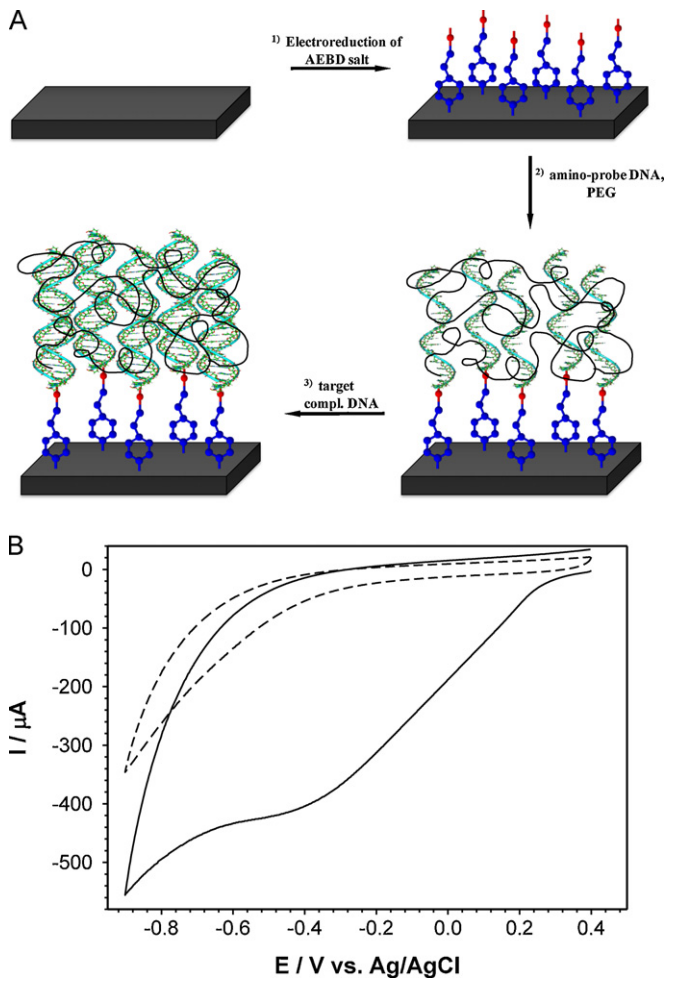

Fig. 1. (A) Scheme of entire procedure of preparation of DNA sensor. (B) Cyclic voltammograms, first (solid line) and fifth (dashed line) cycles, obtained in 2 mM AEBD salt in ACN with addition of 0.1 M NBu_4BF_4. Glassy carbon disc electrode (ϕ = 3 mm); scan rate 100 mV/s.

3.2. Probe immobilization (2)

After the grafting step the electrode was rinsed with ultrapure water, and was slowly dried with argon. Then a 6-μl droplet containing the PEG cross-linker (2 μl of a 15 mg/ml aqueous solution), amino-probe DNA (2 μl of a 400 μg/ml aqueous solution) and 2 μl of water were placed onto the electrode surface to form the sensing layer. Next, the electrode was equilibrated in a dessicator for at least 48 h. From our earlier studies we know that the above ratio of the components guarantees the formation of the best sensing layers (Hajdukiewicz et al., 2009; Kavanagh and Leech, 2006).

3.3. Hybridization (3)

The glassy carbon disc electrodes with the sensing layers were cycled in the potential range $0 \div 0.45 \div 0$ V in a 0.02 M phosphate buffer solution (pH = 7.4) containing 0.15 M NaCl until the voltammograms reached a desired, reproducible signal. Then, the electrodes were rinsed with ultrapure water and dried with argon. The hybridization was performed by placing a 7-μl droplet of the hybridization buffer solution (0.02 M phosphate buffer, pH = 7.4, 1 M NaCl and 1 mM EDTA) containing the target DNA and waiting for 40 min. During that time the drop was protected against rapid evaporation. After completing this step the electrode was carefully washed with phosphate buffer. The same procedure as above was used to check the hybridization progress with the non complementary and mismatch sequences. Additional experiments were done to prove that the hybridization performed with a 7-μl droplet was equivalent to that done with a solution through immersion.

3.4. Impedance transduction

Finally, to perform impedance measurements, the electrode was immersed in a solution of the following composition: 0.02 M phosphate buffer, pH = 7.4, 150 mM NaCl, 5 mM $Fe(CN)_6^{3-}$ and 5 mM $Fe(CN)_6^{4-}$.

4. Results and discussion

Since the major task in the sensor construction was the immobilization of ssDNA through a cross-linker at modified glassy carbon electrode surface, we start with the results related to the successful modification of the glassy carbon surface with AEBD salt.

4.1. Immobilization platform

An acetonitrile solution containing 2 mM AEBD salt was used for the electrochemical reduction of the $-N_2^+$ groups and obtaining the AEBD-terminated GC. Five reduction cycles are sufficient to completely cover glassy carbon surface with organic layer. Typical cyclic voltammograms performed at a GC electrode in an ACN solution containing 2 mM AEBD salt are shown in Fig. 1B.

The quality of GC surface modification by the AEBD salt was examined by applying Raman Spectroscopy, AFM and the measuring of the contact angle. Raman spectra recorded for the AEBD solid salt, bare GC and the gold coated with AEBD electrochemically attached to the GC surface are presented in Figs. 1S and 2S in Supporting Information. The results of the Raman measurements reveal that the aryl groups cover evenly the electrode surface. Anyhow, these results illustrate only the distribution of AEBD at the GC substrate, while the AFM images provide also direct information on the topography of the sample. The AFM images show that the deposited AEBD layer on the GC surface is really uniform, see Fig. 3S in Supporting Information. This is in agreement with the contact angle measurements. The observed stability of the value of the contact angle at grafted electrodes ($21^\circ \pm 4^\circ$) eliminates the possibility of aggregation of AEBD. The hydrophobic carbon became hydrophilic after such modification.

4.2. Impedance response of the modified GC electrode

Impedance measurements were performed in PBS buffer solution containing ferricyanide and ferrocyanide anions in equimolar ratio at open circuit potential. This approach allowed us to measure impedance at equilibrium potential independently of the formal potential of the redox couple. For the bare glassy carbon electrode and also for all tested layers the Nyquist plots consisted of a semicircle followed by a straight line of the slope 45° indicating a simple redox process under kinetic and diffusion control. Exemplary Nyquist plots are shown in Figs. 2 and 3; the Bode-phase angle plots are shown in the insets in Fig. 3. Impedance of the system can be described with a simple Ershler–Randles equivalent circuit, in which capacity of the double layer was replaced by the constant phase impedance CPE_{dl} (see inset in Fig. 2):

$$Z_{CPE} = T^{-1}(i\omega)^{-\phi} = \frac{\cos(\phi\pi/2)}{\omega^{\phi}T} - i\frac{\sin(\phi\pi/2)}{\omega^{\phi}T} \quad (2)$$

where $i = \sqrt{-1}$, $\omega = 2\pi f$, and T represents a proportionality (frequency independent) constant with physical meaning determined by the walue of expotential factor ϕ. Constant phase element represents here a "leaking" and thus not ideal capacitor, which has

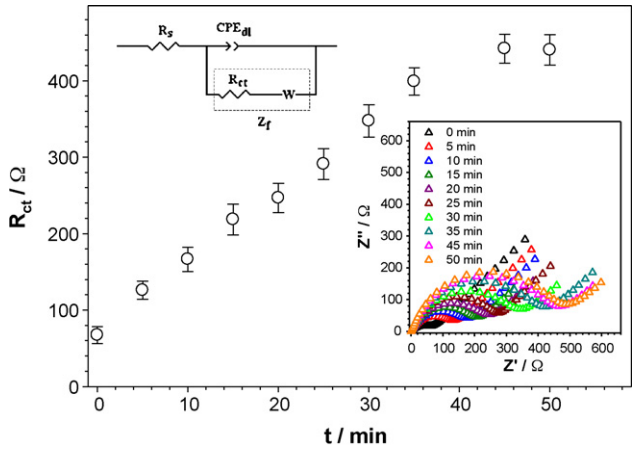

Fig. 2. Plot of R_{ct} (electron transfer resistance) versus hybridization time. Inset I: Nyquist plots obtained for different hybridization times. Inset II: Ershler–Randles equivalent circuit with double layer capacity replaced with constant phase element (CPE_{dl}). R_s – solution resistance, R_{ct} – charge transfer resistance, W – Warburg impedance. Conditions: 0.02 M phosphate buffer (pH 7.4) containing: 0.15 M NaCl, 5 mM $[Fe(CN)_6]^{3-}$ and 5 mM $[Fe(CN)_6]^{4-}$. E_{app} = 245 mV, glassy carbon disc electrode (ϕ = 3 mm), T = 22 °C.

a non-zero real component corresponding to energy dissipation (Lasia, 2009). Only for monocrystalline (or liquid) electrodes in the absence of specific adsorption $\phi = 1$ and purely capacitive behavior is observed; $T \equiv C$. The exponent parameter ϕ is usually smaller than 1, yet the mean capacity of the double layer may be estimated according to the Brug formula (Brug et al., 1984):

$$\overline{C}_{dl} = T^{1/\phi}\left(\frac{1}{R_s} + \frac{1}{R_{ct}}\right)^{1-1/\phi} \quad (3)$$

It should be stressed here that the notation 'double layer' is a simplification, since the nature of the interface with DNA covalently linked to electrode surface is more complex (Yang et al., 2004). Faradaic impedance, Z_f, of the electrode process is a serial connection of the charge transfer resistance and the Warburg impedance related to the diffusion of the electroactive species (redox probe) and may be expressed as:

$$Z_f = R_{ct} + \sigma\omega^{-1/2} - i\sigma\omega^{-1/2} \quad (4)$$

where σ is the Warburg parameter. For a reversible electrode reaction at equilibrium potential

$$\sigma = \frac{RT}{n^2F^2\sqrt{2}}\left(\frac{1}{\sqrt{D_O}C_O^*} + \frac{1}{\sqrt{D_R}C_R^*}\right) \quad (5)$$

D_O, D_R, C_O and C_R denote the diffusion coefficients and the bulk concentrations of both oxidized and reduced forms of the redox species.

Total impedance of the system is described by:

$$Z_{tot} = R_s + \left((i\omega)^{\phi}T + \frac{1}{R_{ct} + \sigma\omega^{-1/2} - i\sigma\omega^{-1/2}}\right)^{-1} \quad (6)$$

The solution resistance, R_s, for all measurements, was equal circa 6 Ω cm^2. Other parameters values for the bare glassy carbon electrode and its consecutive modifications, according to Fig. 1A, are summarized in Table 1. For all measurements the concentration of the redox probe and the buffer solution were kept constant. From Table 1 it follows that the modification of GC electrode by the electroreduction of AEBD salt (step 1 in Fig. 1A) results in a significant increase in the capacity of the double layer C_{dl}. This may indicate that the grafted amino groups are protonated and form a positively charged film at the electrode surface. The protonation of the covalently bound AEBD salt at pH = 7.4 was also suggested by Griveau et al. (Griveau et al., 2007). The formation of a positively charged film contributes also to a decrease of the charge transfer resistance of a negatively charged redox probe. Furthermore, that substantial decrease suggests that the redox process takes place at the close vicinity of the electrode with electron tunneling via aromatic amine rather than directly at the bare glassy electrode surface. The electroreduction of the AEBD salt leads also to a significant decrease in the exponential factor of the CPE parameter. This may indicate that the current distribution at the electrode surface is less uniform. The addition of another time constant is rather unnecessary, since the modification of the equivalent circuit by introduction of an additional resistance parallel to the double layer CPE, representing the redox processes of the layer itself, although, did improve the fitting, did not change the exponential parameter ϕ nor the capacitance of the double layer C_{dl}. The values of this resistance were at least 2 orders of magnitude higher than R_{ct}, so for simplicity we analyzed the data only with the model shown in Fig. 2. A subsequent surface modification with a DNA layer (step 2 in Fig. 1A) improves the

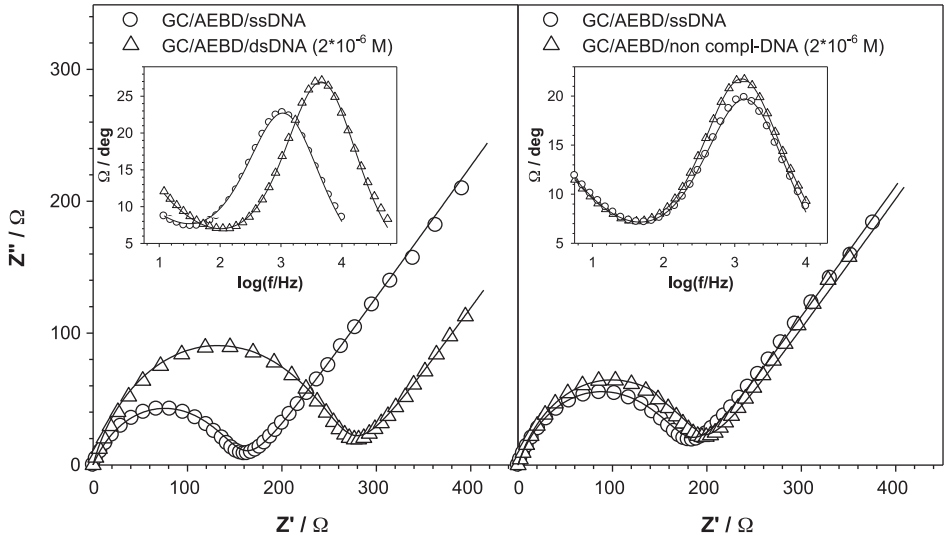

Fig. 3. Complex impedance plot of the modified (GC/AEBD/probe NH_2-ssDNA/compl. target DNA in concentration 2×10^{-6} M and GC/AEBD/probe NH_2-ssDNA/non compl. target DNA in concentration 2×10^{-6} M) glassy carbon disc electrode in the presence of 5 mM $[Fe(CN)_6]^{3-}$ and 5 mM $[Fe(CN)_6]^{4-}$ in 0.02 M phosphate buffer (pH 7.4). Solid lines are fitted to experimental data (points). Insets: Phase angle plots before and after hybridization. Other conditions as in Fig. 2.

Table 1
Changes in impedance parameters (capacitive parameter (T) and exponential factor (ϕ) of constant phase element (CPE); resistance of the charge transfer (R_{ct}), Warburg parameter (σ), and double layer capacity (C_{dl})) during subsequent steps (1, 2, 3) of glassy carbon electrode modification according to Fig. 1A.

EIS parameters	Bare GC	[1)]GC/AEBD	[2)]GC/AEBD/ssDNA	[3)]GC/AEBD/dsDNA[a]
T ($\mu F\, s^{(1-\phi)}\, cm^{-2}$)	10.8 ± 0.1	44 ± 2	32 ± 2	22.9 ± 0.3
ϕ	0.941 ± 0.001	0.854 ± 0.006	0.88 ± 0.01	0.914 ± 0.002
R_{ct} ($\Omega\, cm^2$)	70.3 ± 0.1	16.8 ± 0.2	11.2 ± 0.2	18.4 ± 0.05
σ ($\Omega\, rad^{1/2}\, s^{-1/2}\, cm^2$)	27.8 ± 0.2	31.0 ± 0.1	33.3 ± 0.1	31.6 ± 0.05
C_{dl} ($\mu F\, cm^{-2}$)	5.86 ± 0.06	10.8 ± 0.6	9.4 ± 0.9	10.1 ± 0.2

[a] Concentration of the target DNA was 2×10^{-6} M.

exponential parameter ϕ of the CPE and leads to a further decrease in the resistance of the charge transfer. This may suggest a rather low DNA surface coverage; however, a possibility of DNA-mediated charge transport cannot be excluded (Kelley et al., 1999). The further increase of the CPE exponent ϕ may suggest also structural changes within the layer that lead to a more ordered coating.

The electrostatic repulsions between the redox probe and the negatively charged backbone increases considerably for double stranded DNA (step 3 in Fig. 1A), so the DNA hybridization leads to a significant increase in the charge transfer resistance. The decrease in the capacitive parameter T is balanced with a further increase in the exponential factor ϕ and as a result the electrode capacitance remains unchanged. It is worth of noting, that upon surface modification the Warburg parameter σ remains nearly constant, which suggests that the diffusion process is little influenced by the steric hindrance.

Since the hybridization process is the most important for the scope of this paper, in next sections we will focus on the monitoring of the charge transfer resistance, R_{ct}, as this parameter is apparently most influenced by the hybridization process.

4.3. EIS characterization of the sensing layer

Before impedance measurements the electrodes were cycled in the potential range $0 \div 0.45 \div 0$ V vs. Ag/AgCl in a solution containing 0.02 M phosphate buffer, pH = 7.4, and 0.15 M NaCl until a stable voltammogram was obtained. Fig. 2 shows typical faradaic impedance spectra of the sensing layer in that solution containing additionally the $Fe(CN)_6^{3-/4-}$ redox couple. The spectra were obtained after different hybridization times with fully complementary target DNA. Clearly, the electron transfer resistance (R_{ct}) increased gradually with increasing hybridization time. After 45 min R_{ct} reached a constant, final value, indicating that the hybridization process was completed and the system reached the equilibrium.

4.4. DNA hybridization and EIS detection

Fig. 3 shows the impedance plots registered at the open circuit potential before and after hybridization with completely complementary and non-complementary target DNA. One more impedance spectrum is presented in Figure 4S in Supporting Information. A decrease in the concentration of the target DNA in the droplet caused a decrease in the value of the relative electron transfer resistance (ΔR_{ct}) defined as

$$\Delta R_{ct} = R_{ctdsDNA} - R_{ctssDNA} \quad (7)$$

We turned to the relative electron transfer resistance, because five GC electrodes that were employed in the studies could differ in the surface properties.

Faradaic impedance allows also to get better insight into the quality of the layers; on disordered coatings usually lower CPE exponent and lower fit quality is observed as a result of the frequency-dependent distribution of circuit elements or time-variant behavior. As it is seen in inset in Fig. 3, for the layer with single or double stranded DNA at the electrode surface the impedance data can be satisfactorily fitted to the simple Ershler–Randles model. This means that the employed by us way of the construction of the sensing layer via an AEBD salt leads to high quality layers already at the step of the construction of the sensing layer compared to those obtained by applying the chemisorption of the thiol-modified DNA (Kowalczyk et al., 2010). Using the thiolated DNA sequences such quality is obtained only after the hybridization process. Additionally, to get the appropriate distribution of ssDNA in the sensing layer the mixed alkanothiol monolayer containing HS-R and HS-ssDNA must be used (Levicky et al., 1998).

4.5. Analytical performance

The stability of the biosensor was examined by measuring the changes in the value of the electron transfer resistance of ferricyanide/ferrocyanide couple in PBS buffer every 2 h during the lab hours for 7 days. The response of the sensor was practically unchanged (standard deviation was circa 1.9%) during the first 3 days, and changed to the level of ~74% of the initial response after 7 days. Good stability of the biosensor can be attributed to the good biocompatibility of the AEBD linker and strong covalent interactions between this linker and the sensing film containing: cross-linker (PEG) and amine-terminated capture probe-DNA.

For all applied concentrations (2×10^{-5} to 2×10^{-13} M) the repeatability was good; the relative standard deviation was circa 7% ($n = 4$, two DNA samples). The electrode-to-electrode reproducibility was also examined between five different electrodes in the PBS buffer, and the relative standard deviation was calculated to be 5.2%.

The calibration curves (steady state current vs. target DNA concentration) are shown in Fig. 4. The electron transfer resistance varies with the concentration (increases linearly with log[DNA])

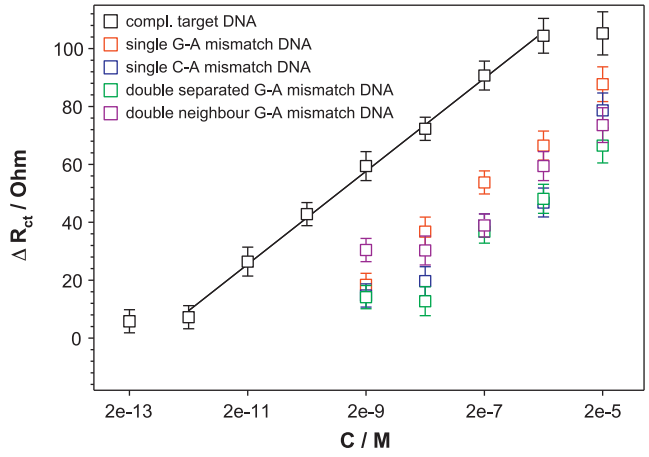

Fig. 4. Plots of difference between the charge transfer resistance (ΔR_{ct}) measured at electrodes modified with ssDNA and dsDNA (partially hybridized ssDNA) vs. concentration (logarithmic scale) of the complementary target-DNA sequences in 7-μl droplets. Other conditions as in Fig. 2.

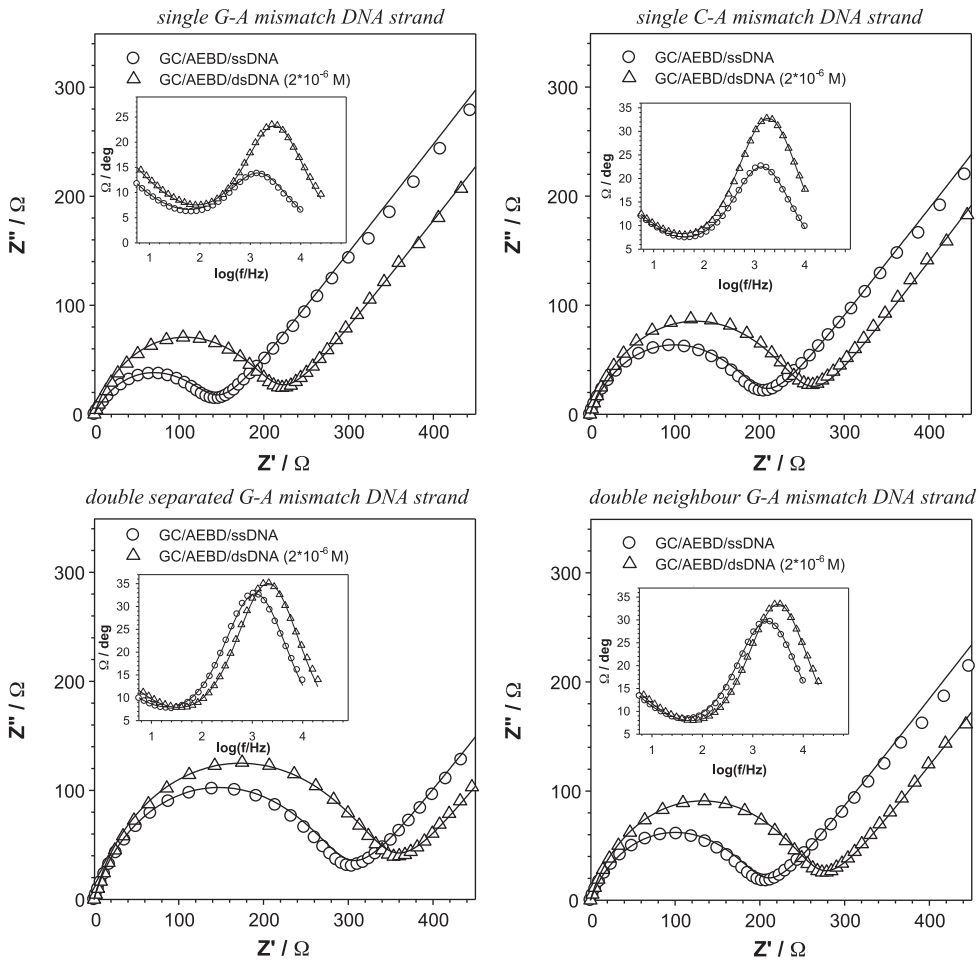

Fig. 5. Impedance plots of the modified glassy carbon disc electrode (GC/AEBD/probe NH_2-ssDNA/mismatch DNA chains in concentration 2×10^{-6} M) in the presence of 5 mM $[Fe(CN)_6]^{3-}$ and 5 mM $[Fe(CN)_6]^{4-}$ in 0.02 M phosphate buffer (pH 7.4). Solid lines are fitted to experimental data (points). Insets: Phase angle plots before and after hybridization.

of complementary target DNA sequences in the range 2×10^{-5} to 2×10^{-13} M. The obtained quantification limit (QL) was circa 6.5×10^{-17} mol in a 7 μl droplet and corresponds to a concentration of 9.2×10^{-12} M of target DNA in the sample. QL was estimated from the equation of the best-fit line of the calibration curve in the range $2 \times 10^{-6} \div 2 \times 10^{-12}$ M and the relative electron transfer resistance (ΔR_{ct}) for the average of the controls using non-complementary target DNA plus 10 times the standard deviations of the controls. This limit is equivalent to the detection of circa 4×10^7 copies of DNA in the 7 μl droplet or circa 5.7×10^{12} DNA copies in a one-liter sample.

4.6. Consequences of base mismatches

As we have mentioned above, EIS can be used to examine the layer morphology at the electrode. The diffusion of the electroactive species is additionally hindered by the dense and tidy layer. It means that the electron transfer resistance should be sensitive to base mismatches and lesions. The EIS spectra for all used mismatch chains are shown in Fig. 5. For all mismatch DNA sequences the relative electron transfer resistance (ΔR_{ct}) decreases compared to full complementary target DNA. However this decrease strongly depended on the type of the mismatch. The presence of mismatches may cause structural alterations including local double helix unwinding. In consequence the sensor layer with double stranded DNA may form the bed-order with many molecular defects. In such the case the redox species present in the solution could easily penetrate the sensor layer, which is reflected by a decrease in ΔR_{ct}. We have noticed that if a mismatch is placed either in the beginning or the end of the chain the resistance effect is apparently smaller. Then the electroactive probe cannot penetrate better the sensing layer.

The molecular defects in the biosensor layer were also controlled through measuring the value of the affinity constant (K_a). The affinity constant for full complementary target DNA is 6.63×10^7 M^{-1}. The biggest damage to the regularity of the layer and in consequence to the electron transfer rate is caused by double separated G-A mismatch DNA strand (K_a circa 0.87×10^6 M^{-1}). The G-A mismatch is the most thermodynamically stable mismatch, being well-stacked within the duplex but under greater dynamic motion than well-paired bases (Luxon and Gorenstein, 1995; Peyret et al., 1999). In the case of the double neighbour G-A mismatch DNA strand, K_a is 1.3×10^6 M^{-1}. For the single mismatches the data show that the electron transfer was not sufficiently sensitive to distinguish between types of mismatches. The affinity constant values were circa 2.7×10^6 and 2.5×10^6 M^{-1} for single G-A mismatch DNA and single C-A mismatch DNA, respectively.

5. Conclusions

The results presented in this paper characterize the binding process of oligonucleotides on the organic layer attached to the glassy carbon electrode surface. Using a monolayer of a diazonium salt covalently attached through electroreduction to the glassy carbon

surface we have constructed a simple, label-free electrochemical DNA biosensor. The organic monolayer as the binder for amino-modified probe DNA provides a good density and distribution of probe DNA in the sensing layer, and in consequence, enough freedom for the coiling process which helps to achieve the highly efficient hybridization. The electrochemical impedance detection based on the measurement of the electron transfer resistance of the ferrocyanide/ferricyanide system with such immobilized DNA sensing layer. Comparing with existing methods for DNA detection, the method described in this paper is very simple (since R_{ct} can be easily estimated from the complex plane plot even without CNLS fitting), sensitive, label-free and can be useful for practical applications. So far the lowest detection limit for the label-free electrochemical detection via EIS was 5×10^{-11} M (Sassolas et al., 2008).

Acknowledgements

Support for this work by the Polish Ministry of Science and Higher Education Grant N N204 244534 is gratefully acknowledged.

Appendix A. Supplementary data

Supplementary data associated with this article can be found, in the online version, at doi:10.1016/j.bios.2010.10.046

References

Actis, P., Caulliez, G., Shul, G., Opallo, M., Mermoux, M., Marcus, B., Boukherroub, R., Szunertis, S., 2008. Langmuir 24, 6327–6333.
Adenier, A., Chehimi, M.M., Gallardo, I., Pinson, J., Vilà, N., 2004. Langmuir 20, 8243–8253.
Brug, G.J., Van Den Eeden, A.L.G., Sluyters-Rehbach, M., Sluyters, J.H., 1984. J. Electroanal. Chem. 176, 275–295.
Campbell, C.N., Gal, D., Cristler, N., Banditrat, C., Heller, A., 2002. Anal. Chem. 74, 158–162.
Caruana, D.J., Heller, A., 1999. J. Am. Chem. Soc. 121, 769–774.
Downard, A.J., 2000. Electroanalysis 12, 1085–1096.
Erdem, A., Kerman, K., Meric, B., Akarca, U.S., Ozsoz, M., 1999. Elrctroanalysis 11, 586–588.
Gallardo, I., Pinson, J., Vilà, N., 2006. J. Phys. Chem. B 110, 19521–19529.
Ghanem, M.A., Chrétien, J.-M., Kilburn, J.D., Bartlett, P.N., 2009. Bioelectrochemistry 76, 115–125.
Griveau, S., Mercier, D., Vautrin-Ul, Ch., Chaussé, A., 2007. Electrochem. Commun. 9, 2768–2773.
Gu, T., Hasebe, Y., 2006. Biosens. Bioelectron. 21, 2121–2128.
Hajdukiewicz, J., Boland, S., Kavangh, P., Nowicka, A., Stojek, Z., Leech, D., 2009. Electroanalysis 21, 342–350.
Hashimoto, K., Ito, K., Ishimori, Y., 1994. Anal. Chim. Acta 286, 219–224.
Kambhampati, D., Nielsen, P.E., Knoll, W., 2001. Biosens. Bioelectron. 16, 1109–1118.
Kavanagh, P., Leech, D., 2006. Anal. Chem. 78, 2710–2716.
Kelley, S.O., Jackson, N.M., Hill, M.G., Barton, J.K., 1999. Angew. Chem. Int. Ed. 38, 941–945.
Kowalczyk, A., Nowicka, A.M., Jurczakowski, R., Niedzialkowski, P., Ossowski, T., Stojek, Z., 2010. Electroanalysis 22, 49–59.
Lasia, A., 2009. In: Schlesinger, M. (Ed.), Modern Aspects of Electrochemistry. Springer, pp. 67–138.
Levicky, R., Herne, T.M., Tarlov, M.J., Satija, S.K., 1998. Am. Chem. Soc. 120, 9787–9792.
Lin, X., Kang, G., Lu, L., 2007. Bioelectrochemistry 70, 235–244.
Liu, J., Tian, S., Nielsen, P.E., Knoll, W., 2005. Chem. Commun. 23, 2969–2971.
Luxon, B.A., Gorenstein, D.G., 1995. Methods Enzymol. 261, 45–73.
Marrazza, G., Chianella, I., Mascini, M., 1999. Biosens. Bioelectron. 14, 43–51.
Neumann, T., Johansson, M.L., Kambhampati, D., Knoll, W., 2002. Adv. Funct. Mater. 12, 575–586.
Palecek, E., Jelen, F., Teijeiro, C., Fucik, V., Jovin, T.M., 1993. Anal. Chim. Acta 273, 175–186.
Peyret, N., Seneviratne, P.A., Allawi, H.T., Santa Lucia, J., 1999. Biochemistry 38, 3468–3477.
Pinson, J., Podvorica, F., 2005. Chem. Soc. Rev. 34, 429–439.
Pividori, M.I., Merkoci, A., Alegret, S., 2000. Biosens. Bioelectron. 15, 291–303.
Sassolas, A., Leca-Bouvier, B.D., Blum, L.J., 2008. Chem. Rev. 108, 109–139.
Tanaka, H., Aramata, A., 1997. J. Electroanal. Chem. 437, 29–35.
Wang, J., Cai, X., Rivas, G., Shiraishi, H., Farias, P.A.M., Dontha, N., 1996. Anal. Chem. 68, 2629–2634.
Yang, W., Butler, J.E., Russell Jr., J.N., Hamers, R.J., 2004. Langmuir 20, 6778–6787.